

Phase diffusion and locking in single-qubit lasers

Stephan André,¹ Valentina Brosco,^{1,2} Alexander Shnirman,^{3,4} and Gerd Schön^{1,4}

¹*Institut für Theoretische Festkörperphysik, Universität Karlsruhe, 76128 Karlsruhe, Germany*

²*Dipartimento di Fisica, Università “La Sapienza”, P.le A. Moro 2, 00185 Roma, Italy*

³*Institut für Theorie der Kondensierten Materie,
Universität Karlsruhe, 76128 Karlsruhe, Germany*

⁴*DFG Center for Functional Nanostructures (CFN),
Universität Karlsruhe, 76128 Karlsruhe, Germany*

Motivated by recent experiments, which demonstrated lasing and cooling of the electromagnetic field in an electrical resonator coupled to a superconducting qubit, we study the phase coherence and diffusion of the system in the lasing state. We also discuss phase locking and synchronization induced by an additional *ac* driving of the resonator. We extend earlier work to account for the strong qubit-resonator coupling and to include the effects of low-frequency qubit’s noise. We show that the strong coupling may lead to a double peak structure of the spectrum, while the shape and width are determined to the low-frequency noise.

PACS numbers:

In a number of recent experiments (here we only cite few examples) superconducting qubits coupled on chip to electrical or mechanical resonators displayed quantum electrodynamic effects and opened the field of “circuit QED” [1–9]. By creating a population inversion between two charge states in a driven superconducting single-electron transistor (SSET) Astafiev *et al.* [8] demonstrated lasing behaviour of a microstripline resonator coupled to the qubit. Grajcar *et al.* [9] coupled a driven flux qubit to a low-frequency *LC* resonator and observed both cooling and a trend towards lasing of the resonator field. In contrast to usual lasers, where many atoms are weakly coupled to the electromagnetic field, in single-qubit lasers one artificial atom is coupled strongly to the resonator. In addition, solid state qubits are subject to decoherence effects. Some of the consequences and novel behavior had been analyzed in Refs. [10–15].

Even in the lasing state, the coherence of the electromagnetic field is lost due to phase diffusion after a characteristic time τ_d [16], an effect which is observable, e.g., in the laser spectrum. Phase diffusion can be suppressed by *injection locking*, that is by driving the resonator with an additional coherent signal. This fixes the phase difference between the laser and driving field to a value which depends on the intensity and detuning of the latter. Both injection locking and phase diffusion were studied experimentally for a single-qubit laser in Ref. [8]. As compared to the spectrum observed in standard (many-atom) lasers, the single-qubit laser spectrum is broader and the peak is substantially shifted with respect to the natural resonator frequency. The maximum photon number in the resonator is rather low, raising questions about the coherent nature of the amplification in these systems.

In this work we study the spectral properties of single-qubit lasers and explain qualitatively several of the experimental observations. In Section I we introduce the model and describe our approach. Results for static properties of single qubit lasers are discussed in Section II. Here we focus on the average photon number in the vicinity

of the lasing transition, which illustrates the differences between single- and multi-atom lasers. We show explicitly that single qubit lasers are characterized by a smooth transition to the lasing regime and by the absence of a sharp lasing threshold. Next, in Section III, we analyze the phase diffusion of the resonator field focusing on the following issues: (i) we discuss the effects of correlations between qubit and resonator on the diffusion process; (ii) we show how the interplay between strong coupling and spontaneous emission may lead to a double peak structure in the spectrum; and (iii) we demonstrate how low-frequency noise leads to inhomogeneous broadening of the lasing peak. Finally, in Section IV, we study injection locking induced by an external coherent driving, we discuss the main features of the spectrum, and we provide an estimate for the locking threshold.

I. MODEL

We consider a single-mode quantum resonator coupled to N_a qubits (labelled by μ) and we account for both resonator and qubit dissipation. In the rotating wave approximation the system is described by the Hamiltonian

$$H = \hbar\omega_0 a^\dagger a + \frac{1}{2}\hbar\omega_p \sum_{\mu} \sigma_z^\mu + \hbar g \sum_{\mu} (\sigma_+^\mu a + \sigma_-^\mu a^\dagger) \quad (1) \\ + (a + a^\dagger)X_a + \sum_{\mu} (X_z^\mu \sigma_z^\mu + X_+^\mu \sigma_+^\mu + X_-^\mu \sigma_-^\mu) + H_N.$$

Apart from the photon operators, a and a^\dagger , we introduced the Pauli matrices acting on the single-qubit eigenstates $\sigma_z^\mu = |1_\mu\rangle\langle 1_\mu| - |0_\mu\rangle\langle 0_\mu|$, $\sigma_+^\mu = |1_\mu\rangle\langle 0_\mu|$, $\sigma_-^\mu = |0_\mu\rangle\langle 1_\mu|$. Dissipation is modelled by assuming that the oscillator and the qubits interact with noise operators, X_a and X_z^μ , X_+^μ , X_-^μ , belonging to independent baths with Hamiltonian H_N in thermal equilibrium. The noise coupling longitudinally to the qubits, $X_z^\mu \sigma_z^\mu$, is re-

sponsible for the qubits' pure dephasing. To describe lasing, we assume that a population inversion has been created in the qubits, which we describe by assuming that the effective temperature of the qubit baths is negative. In this way (for $N_a = 1$) we model the essential properties of the SSET laser used by Astafiev *et al.* [8, 14]. Possible deviations from the standard Jaynes-Cummings oscillator-qubit coupling used in Eq. (1) are discussed in Appendix A. From the Hamiltonian (1), following the route described, e.g., in Ref. [16], we derive a set of quantum Langevin equations of motion,

$$\begin{aligned} \frac{d}{dt}\sigma_z^\mu &= -2ig(\sigma_+^\mu a - \sigma_-^\mu a^\dagger) - \Gamma_1(\sigma_z^\mu - D_0) + F_z^\mu(t), \\ \frac{d}{dt}\sigma_+^\mu &= -(\Gamma_\varphi - i\omega_p)\sigma_+^\mu - ig\sigma_z^\mu a^\dagger + F_+^\mu(t), \\ \frac{d}{dt}a &= -\left(\frac{\kappa}{2} + i\omega_0\right)a - ig\sum_\mu \sigma_-^\mu + F_a(t). \end{aligned} \quad (2)$$

Here the rate $\Gamma_1 = \Gamma_\downarrow + \Gamma_\uparrow$ is the sum of excitation and relaxation rates, while $\Gamma_\varphi = \Gamma_1/2 + \Gamma_\varphi^*$ is the total dephasing rate, which also accounts for pure dephasing due to the longitudinal noise described by Γ_φ^* . In contrast to relaxation and excitation processes, Γ_φ^* accounts for processes with no energy exchange between qubit and environment, which thus do not affect the populations of the two qubit states. Furthermore, κ is the bare resonator damping. The parameter $D_0 = (\Gamma_\uparrow - \Gamma_\downarrow)/\Gamma_1$ denotes the stationary qubit magnetization in the absence of the resonator. In the present case, since we assume a negative temperature of the qubits baths and a population inversion we have $D_0 > 0$. The Langevin operators $F_i^\mu(t)$ with $i = +, -, z$ have vanishing averages and are characterized by their correlation functions, $\langle F_i^\mu(t) F_j^\nu(t') \rangle = \delta_{\mu\nu} D_{ij}^\mu g_q(t - t')$. The function $g_q(t - t')$ is assumed to decay on a time scale much shorter than the relaxation and decoherence times of the qubits and the oscillator. The diffusion coefficients D_{ij}^μ are related to the rates introduced above, $D_{+-}^\mu = \Gamma_\uparrow + \Gamma_\varphi^*(1 + \langle \sigma_z^\mu \rangle)$, $D_{-+}^\mu = \Gamma_\downarrow + \Gamma_\varphi^*(1 - \langle \sigma_z^\mu \rangle)$, $D_{zz}^\mu = 2\Gamma_1 - 2(\Gamma_\uparrow - \Gamma_\downarrow)\langle \sigma_z^\mu \rangle$, $D_{z+}^\mu = 2\Gamma_\downarrow\langle \sigma_+^\mu \rangle$, $D_{z-}^\mu = -2\Gamma_\uparrow\langle \sigma_-^\mu \rangle$. Similarly, the Langevin force $F_a(t)$ acting on the resonator with $\langle F_a^\dagger(t) F_a(t') \rangle = \kappa N_{th} g_a(t - t')$ is characterized by the rate κ and thermal photon number N_{th} . The qubit and oscillator noises are assumed to be independent. For a further discussion of the different rates and diffusion coefficients we refer to standard quantum optics textbooks, e.g. Ref. [17].

II. STATIC PROPERTIES

By taking appropriate products of Eqs. (2) and performing averaging, we arrive at the following equations for the average photon number, $\langle n \rangle$, the qubit polarization $\langle \sigma_z^\mu \rangle$ and the product $\langle \sigma_+^\mu a \rangle$:

$$\frac{d}{dt}\langle \sigma_z^\mu \rangle = -2ig(\langle \sigma_+^\mu a \rangle - \langle \sigma_-^\mu a^\dagger \rangle) - \Gamma_1(\langle \sigma_z^\mu \rangle - D_0) \quad (3)$$

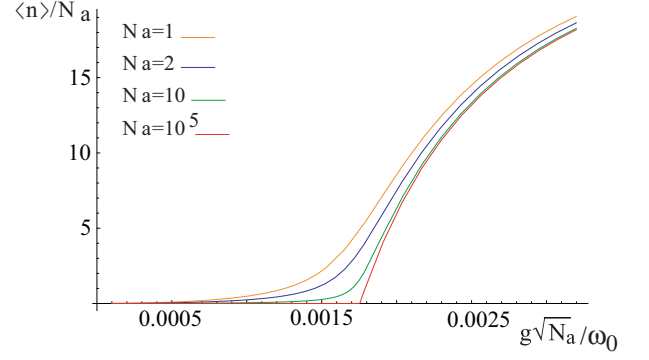


Figure 1: Color online - Scaled photon number, $\langle n \rangle / N_a$, in the threshold region versus scaled coupling, $g\sqrt{N_a}$ for different values of N_a . The other parameters are: $\omega_p = \omega_0$, $\Gamma_1/\omega_0 = 0.016$, $\Gamma_\varphi^*/\omega_0 = 0.004$, $D_0 = 0.975$, $\kappa/\omega_0 = 3 \cdot 10^{-4}$ and $N_{th} = 0$.

$$\begin{aligned} \frac{d}{dt}\langle n \rangle &= ig \sum_\mu (\langle \sigma_+^\mu a \rangle - \langle \sigma_-^\mu a^\dagger \rangle) - \kappa(\langle n \rangle - N_{th}), \quad (4) \\ \frac{d}{dt}\langle \sigma_+^\mu a \rangle &= (i\Delta - \gamma)\langle \sigma_+^\mu a \rangle - ig\langle \sigma_z^\mu n \rangle - i \sum_\nu \langle \sigma_+^\mu \sigma_-^\nu \rangle, \end{aligned} \quad (5)$$

where we introduced the detuning $\Delta = \omega_p - \omega_0$ and the total dephasing rate $\gamma = \Gamma_\varphi + \frac{\kappa}{2}$.

In the stationary limit, neglecting the correlations between different qubits, i.e. assuming $\langle \sigma_+^\mu \sigma_-^\nu \rangle \simeq \delta_{\mu\nu}(1 + \langle \sigma_z^\mu \rangle)$, the previous equations yield the following two exact relations between three quantities, the average polarization $\langle S_z(t) \rangle$ with $S_z \equiv \frac{1}{N_a} \sum_\mu \sigma_z^\mu$, the photon number $\langle n(t) \rangle$, and the correlation function $\langle n S_z \rangle$,

$$\begin{aligned} \langle n \rangle &= N_{th} + \frac{2g^2 N_a}{\kappa} \frac{\gamma}{\gamma^2 + \Delta^2} \left[\langle S_z n \rangle + \frac{\langle S_z \rangle + 1}{2} \right], \\ \langle S_z \rangle &= D_0 - \frac{4g^2}{\Gamma_1} \frac{\gamma}{\gamma^2 + \Delta^2} \left[\langle S_z n \rangle + \frac{\langle S_z \rangle + 1}{2} \right]. \end{aligned} \quad (6)$$

If one of them is known, e.g., from a numerical solution of the Master equation, the other two can readily be determined.

Factorizing the correlator, $\langle S_z n \rangle \approx \langle S_z \rangle \langle n \rangle$, on the right-hand side of Eqs. (6) gives results known in quantum optics as “semi-quantum model” [18]. It includes spontaneous emission processes, described by the term proportional to $(\langle S_z \rangle + 1)$.

Spontaneous emission has a twofold importance for the issues described in the present work. First, at low temperatures it is responsible for the line-width of the lasers. Second, as noticed in Ref. [19], due to the low photon number, spontaneous emission is especially relevant in the description of the dynamics of single atom lasers. To illustrate this fact, we plot in Fig. 1 the scaled photon number $\langle n \rangle / N_a$ as a function of the scaled coupling $g\sqrt{N_a}$ for different values of N_a . The product $g\sqrt{N_a}$ is

kept constant to have a universal asymptotic behaviour. In the limit of large N_a we observe a sharp lasing transition occurring at the threshold coupling $g_{\text{thr}}\sqrt{N_a} = \sqrt{\kappa\gamma/(2D_0)}$, as predicted by the semiclassical theory. On the other hand, for low values of N_a , and in particular for $N_a = 1$, we find a smooth crossover between the normal and the lasing regimes, which is due to spontaneous emission. In this case, although we cannot define a sharp threshold condition, we can still identify a transition region centered at the semiclassical threshold coupling. The results presented in Fig. 1 were obtained analytically using the semi-quantum approximation. In the case $N_a = 1$ we compared such results with the numerical solution of the Master Equation and we obtained an agreement better than 10^{-3} .

III. PHASE DIFFUSION

For typical circuit QED parameters, i.e., for strong coupling g , the semi-quantum approximation, in spite of giving, as explained above, a good estimate of the stationary photon number, cannot be used to study spectral functions. For the analysis of phase diffusion we thus proceed with a *hybrid* approach: starting from Heisenberg equations of motion we derive analytical expressions for the phase correlation time and frequency shift of the lasing peak, both expressed as functions of the single-time averages, i.e., the photon number and qubit inversion in the stationary state. We then use the Master equation for the reduced qubit-resonator density matrix to calculate the single-time averages.

From now on we consider a single-qubit laser, $N_a = 1$, and analyze the laser and cross correlation functions

$$\begin{aligned} O(\tau) &= \lim_{t \rightarrow \infty} \langle a^\dagger(t + \tau) a(t) \rangle, \\ G(\tau) &= \lim_{t \rightarrow \infty} \langle \sigma_+(t + \tau) a(t) \rangle. \end{aligned} \quad (7)$$

Starting from the quantum Langevin equations (2) we derive a hierarchy of equations involving $O(\tau)$ and $G(\tau)$. To truncate the hierarchy we split $a(t)$ into an amplitude and phase, $a(t) = \sqrt{n(t)} e^{-i\varphi(t)}$, and assume that the correlation time of phase fluctuations, $1/\kappa_d$, is much longer than that of amplitude fluctuations, $\sim 1/\kappa$ [16]. This allows us to approximate for sufficiently long times, $\tau > 1/\kappa$,

$$\langle \sigma_z(t + \tau) a^\dagger(t + \tau) a(t) \rangle \simeq \frac{\langle \sigma_z \sqrt{n} \rangle}{\langle \sqrt{n} \rangle} \langle a^\dagger(t + \tau) a(t) \rangle, \quad (8)$$

while the correlator $\langle \sigma_z \sqrt{n} \rangle$ can be estimated as

$$\frac{\langle \sigma_z \sqrt{n} \rangle}{\langle \sqrt{n} \rangle} \simeq \frac{1}{2} \left(\langle \sigma_z \rangle + \frac{\langle \sigma_z n \rangle}{\langle n \rangle} \right). \quad (9)$$

Above threshold this approximation, which neglects terms of order $\langle \delta n^2 \rangle / \langle n \rangle^2$, is justified when the fluctuations of the photon number are much smaller than the

average. Starting from Eqs. (2) and using the factorization (8) we obtain a coupled set of equations,

$$\begin{aligned} \frac{d}{d\tau} O(\tau) &= (i\omega_0 - \frac{\kappa}{2}) O(\tau) + igG(\tau), \\ \frac{d}{d\tau} G(\tau) &= (i\omega_p - \Gamma_\varphi) G(\tau) - ig \frac{\langle \sigma_z \sqrt{n} \rangle}{\langle \sqrt{n} \rangle} O(\tau). \end{aligned} \quad (10)$$

These equations depend implicitly on all the parameters specified above. We focus on the case where the oscillator damping is much weaker than qubit's dephasing, $\kappa/2 \ll \Gamma_\varphi$, which is usually satisfied in single-qubit lasing experiments. In this case we obtain from Eqs. (10) for the oscillator's spectral function, i.e., the real part of the Fourier transform of the correlator $O(\tau)$, a Lorentzian,

$$\hat{O}(\omega) = \frac{2\kappa_d \langle n \rangle}{(\omega - \omega_0 - \delta\omega_0)^2 + \kappa_d^2}. \quad (11)$$

It depends on the phase diffusion rate

$$\begin{aligned} \kappa_d &= \frac{\kappa}{2} \frac{N_{th}}{\langle n \rangle} + \frac{g^2 \Gamma_\varphi}{2 \langle n \rangle} \frac{(\langle \sigma_z \rangle + 1)}{\Gamma_\varphi^2 + \Delta^2} \\ &\quad + \frac{g^2 \Gamma_\varphi}{\Gamma_\varphi^2 + \Delta^2} \frac{\langle \sigma_z n \rangle - \langle \sigma_z \rangle \langle n \rangle}{2 \langle n \rangle}, \end{aligned} \quad (12)$$

and the frequency shift

$$\begin{aligned} \delta\omega_0 &= \frac{\Delta}{2 \langle n \rangle} \left[\frac{\kappa (\langle n \rangle - N_{th})}{\Gamma_\varphi} - g^2 \frac{\langle \sigma_z \rangle + 1}{\Gamma_\varphi^2 + \Delta^2} \right] \\ &\quad - \frac{g^2 \Delta}{\Gamma_\varphi^2 + \Delta^2} \frac{\langle \sigma_z n \rangle - \langle \sigma_z \rangle \langle n \rangle}{2 \langle n \rangle}. \end{aligned} \quad (13)$$

The spectral function $\hat{O}(\omega)$ is proportional to the spectrum measured in Ref. [8]. Equations (12) and (13) are the main results of the present work. Upon factorization of the correlator $\langle \sigma_z n \rangle$ far above and below the lasing transition they reduce to results known from quantum optics [16]. The phase diffusion rate (12) is the sum of three terms. The first represents a thermal contribution to the linewidth and is negligible in the experimental regime explored in Ref. [8]. The second describes the effect of relaxation processes of the qubit, which, due to the strong coupling, strongly increases the linewidth. The third term, due to quantum correlations, is essentially a measure of the coherent coupling between the qubit and the oscillator and leads to a *reduction* of the linewidth. Its effect is illustrated in the inset of Fig. 2, where we plot the diffusion constant κ_d given by (12) covering the whole range from below to above threshold and compare it to the diffusion rate, κ_d^{fac} , obtained by factorizing the correlator $\langle \sigma_z n \rangle$. As one can see correlations give significant quantitative corrections. Furthermore, we note that there is a wide range of parameters in which our approximations remain consistent; in the case of strong coupling g this corresponds indeed to have $\kappa_d < \kappa$ (see discussion around Eq. (8)).

Fig. 2 also displays the dependence of the phase diffusion rate on the pure Markovian dephasing rate Γ_φ^* ,

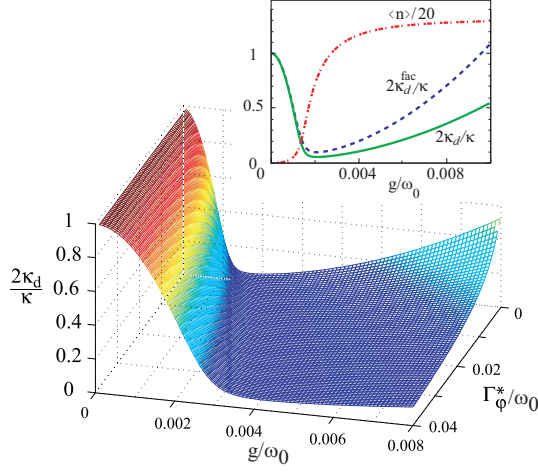


Figure 2: Color online - Diffusion constant versus qubit-oscillator coupling and pure dephasing; parameters as in Fig.1. Inset: phase diffusion constants, κ_d and κ_d^{fac} , calculated with and without taking into account correlation and the average photon number obtained from the Master equation for $\Gamma_\varphi^*/\omega_0 = 0.004$.

showing a reduction of the linewidth with increasing Γ_φ^* above threshold. This surprising feature is a consequence of the fact that pure dephasing processes are not associated with emission of incoherent photons in the resonator, and their main effect is simply a decrease of the effective qubit-resonator coupling. As one notes from the inset of Fig. 2, in single-qubit lasers far above threshold a reduction of the coupling has little effect on the saturated photon number but leads to a decrease of the incoherent photon emission rate, thus diminishing the linewidth.

Another interesting manifestation of this effect is shown in the left panel of Fig. 3. Here we plot the height of the spectral line $\hat{O}(\omega_0 + \delta\omega_0) = \langle n \rangle / \kappa_d$ as a function of the detuning, Δ . One can see that the optimal lasing conditions are realized somewhat out of resonance, where the effective coupling is weaker. We thus observe two peaks in the spectrum symmetrically shifted with respect to $\Delta = 0$. Due to the strong coupling the photon number is roughly constant in the region between the two peaks. A similar structure in the output spectrum of single atom laser was also found in a numerical study by Ginzel *et al.* [20]. One might conjecture that this effect is the origin of the two spots observed in the experiment. It would explain why the peaks do not occur at resonance, but we have not succeeded to fit the experimental data in a satisfactory way [24]. In Ref. [8] it was proposed that the second peak is related to two-photon processes. Indeed deviations from the model used in Eq. (1), lead to an effective two-photon-coupling between the qubit and the resonator. However, as described in the appendix, the two-photon

coupling constant seems to be too small to produce any “two-photon lasing”. This results is also confirmed by the numerical solution of the Master Equation. We also note that in the experiment the second peak appears substantially shifted from the two-photon resonance condition, using the data of Ref. [8], at the second peak we have $2\omega_0 - \omega_p \simeq 0.4\omega_0$.

The linewidth of order of 0.3MHz observed in Ref. [8] is about one order of magnitude larger than what follows from Eq. (12) (of the order of the Schawlow-Townes linewidth). Moreover in the experiment the laser line shows a Gaussian rather than a Lorentzian shape. Both discrepancies may be explained if we note that the qubit’s dephasing is mostly due to low-frequency charge noise, which cannot be treated within the Markov approximation used in the derivation of Eqs.(11)-(13). However, low-frequency (quasi-static) noise can be taken into account by averaging the Lorentzian line in Eq. (11) over different detunings [22]. Assuming that the detuning fluctuations are Gaussian distributed with mean $\bar{\Delta}$ and width σ , such that $\Gamma_1 > \sigma \gg \kappa_d$, we can neglect in the saturated limit the fluctuations of κ_d and $\langle n \rangle$ and assume that the frequency shift $\delta\omega_0$ depends linearly on the detuning Δ . From Eq. (13) we then have $\delta\omega_0 \simeq \Delta\kappa/(2\Gamma_\varphi)$, and we obtain a Gaussian line with width $\tilde{\sigma} \simeq \sigma\kappa/(2\Gamma_\varphi)$, where we remark that Γ_φ is the total markovian dephasing rate. The linewidth observed in the experiment is then reproduced by a reasonable value of σ of order of 300 MHz. In the case in which σ is larger than Γ_1 , the previous formula overestimate the linewidth since it doesn’t take into account the decay of $\langle n \rangle$ out of threshold. In this case one can perform the averaging numerically. Anyway, in the presence of low-frequency noise, the linewidth is governed not by κ_d as one may have expected, but by $\delta\omega_0$.

IV. INJECTION LOCKING

We next investigate the behavior of the single-qubit laser when the oscillator is driven by an external laser field or seed light. To describe monochromatic driving with frequency ω_{dr} and amplitude E_0 , we add a term $E_0 a e^{i\omega_{\text{dr}} t} + \text{H.c.}$ to the Hamiltonian (1). It leaves the equations for the qubit operators unchanged, but modifies the quantum Langevin equation for the resonator,

$$\frac{d}{dt}a = -\left(i\omega_0 + \frac{\kappa}{2}\right)a - iE_0^* e^{-i\omega_{\text{dr}} t} - ig\sigma_- + F_a(t). \quad (14)$$

The average $\langle a \rangle$ now acquires a non-vanishing value and oscillates with the driving frequency ω_{dr} . In the resonant case $\omega_{\text{dr}} = \omega_0 = \omega_p$, we estimate $\langle \tilde{a}^\dagger \rangle \equiv \langle a e^{+i\omega_{\text{dr}} t} \rangle = -iE_0/\bar{\kappa}_d$, where $\bar{\kappa}_d = \frac{1}{2}\left(\kappa_d + \sqrt{\kappa_d^2 + 2|E_0|^2/\langle n \rangle}\right)$ and κ_d has the same functional dependence on $\langle n \rangle$ and $\langle \sigma_z \rangle$ as in the undriven resonant case, $\kappa_d = \frac{\kappa}{4}\left(1 + \frac{N_{\text{th}}}{\langle n \rangle}\right) +$

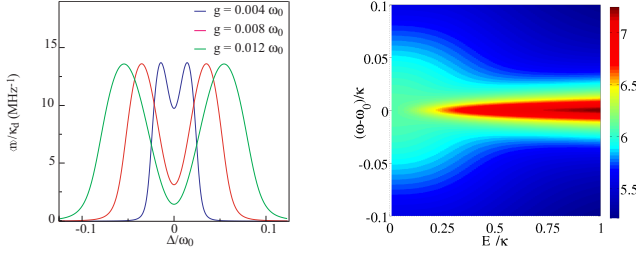


Figure 3: Color online - Left panel: Maximum spectrum's amplitude $\hat{O}(\omega_0 + \delta\omega_0)$ for different values of g . Right panel: Logarithm of the normalized resonator spectrum, $\log[\omega_0 \hat{O}(\omega)]$ in the presence of an external driving at resonance as a function of the driving power. $\omega_0 = 10\text{GHz}$ other parameters as in Fig. 1.

$$\frac{g^2}{2\Gamma_\varphi} \left(\frac{\langle \sigma_z \rangle + 1}{2\langle n \rangle} - \langle \sigma_z \rangle \right).$$

Finally, we consider the emission spectrum of the single qubit laser in the injection locking regime. For simplicity we neglect the low-frequency noise. In the double resonance regime, that is for $\omega_{\text{dr}} = \omega_0 = \omega_p$, we get a simple analytical expressions for $\hat{O}(\omega)$,

$$\hat{O}(\omega) = \frac{2\bar{\kappa}_d (\langle n \rangle - \langle \tilde{a}^\dagger \rangle \langle \tilde{a} \rangle)}{(\omega - \omega_0)^2 + \bar{\kappa}_d^2} + 2\pi\delta(\omega - \omega_0) \langle \tilde{a}^\dagger \rangle \langle \tilde{a} \rangle. \quad (15)$$

For low driving amplitude E_0 , the resonator output is thus the superposition of two signals: the Lorentzian lasing peak and a coherent peak due to the driving proportional to $|\langle \tilde{a} \rangle|^2$. As one can see by combining the previous equation with the expression of $\langle \tilde{a}^\dagger \rangle$, with increasing E_0 , the height of the Lorentzian decreases and approaches zero, while the coherent peak grows. Eventually for large values of E_0 , only the latter, which is amplified due to the coupling to the qubit, is visible in the spectrum. The driving amplitude, \bar{E}_0 , at which the Lorentzian peak disappears can be evaluated, using Eq.(15), as $\bar{E}_0^2 \simeq \langle n \rangle \bar{\kappa}_d^2$. The comparison to the experimental results of Ref. [8] can be done estimating the mean power absorbed by the system, P_d , as follows: $P_d \simeq E_0^2 \omega_0 / \bar{\kappa}_d$ [17]. To illustrate the locking transition we plot in Fig. 3 (right panel) the spectrum (15). The output spectrum is centered at $\omega = 0$ since $\delta\omega_0 = 0$. In the numerics we assumed that the injected signal has a Lorentzian shape with width $w_{\text{dr}} = \kappa/200$. In the presence of a finite qubit-oscillator detuning $\Delta = \omega_p - \omega_0$, the position of the lasing peak would be shifted.

V. CONCLUSION

We analyzed in detail the spectral properties of single-qubit lasers. Our main conclusions are:

- Due to the strong coupling nontrivial structures appear in the spectrum, which are not visible in the average photon number. As shown in Fig. 3 the optimal lasing conditions are realized for two values of the detuning, which

are symmetrically shifted from $\Delta = 0$. At these two hot-spots the output spectrum has the maximum height and it is centered around the frequency $\omega_0 \pm \delta\omega_0$.

- Low-frequency noise strongly affects the line shape of the two peaks, leading to an inhomogeneous broadening. In comparison, the natural laser linewidth due to spontaneous emission is negligible.

- Although we did not produce a quantitative fit to the data, we presented a possible explanation of the double-peak structure observed in the experiment of Ref. [8]. We obtained an estimate of the linewidth due to low frequency noise in qualitative agreement with the experiments, and we evaluated the locking threshold in the injection locking experiment.

We acknowledge fruitful discussions with O. Astafiev, A. Fedorov and M. Marthaler. The work is part of the EU IST Project EUROSQIP

Appendix A

Here we briefly discuss the validity of the model introduced in Section I, when applied to describe the experiment of Astafiev *et al.* [8]. The single-qubit laser realized in Ref. [8], consists of a charge qubit coupled capacitively to a single-mode electrical resonator and can be thus described in the qubit's eigenbasis by the Hamiltonian

$$H = \frac{1}{2} \Delta E \sigma_z + \hbar \omega_0 a^\dagger a - \hbar g_0 (\sin \zeta \sigma_z + \cos \zeta \sigma_x) (a + a^\dagger). \quad (A1)$$

The angle ζ and the qubit energy splitting depend on the charging and Josephson energies, ε_{ch} and E_J , $\tan \zeta = \frac{\varepsilon_{\text{ch}}}{E_J}$ and $\Delta E = \sqrt{\varepsilon_{\text{ch}}^2 + E_J^2}$. In order to identify the one- and two-photon couplings, we now apply a Schrieffer-Wolff transformation $U = e^{iS}$ with $S = i \frac{g_0 \sin \zeta}{\omega_0} \sigma_z (a - a^\dagger)$ and perform a perturbation expansion in the parameter g_0/ω_0 . The transformed Hamiltonian, $\tilde{H} = U^\dagger H U$, thus becomes

$$\begin{aligned} \tilde{H} \simeq & \frac{1}{2} \Delta E \sigma_z + \hbar \omega_0 a^\dagger a + \hbar g_1 \sigma_x (a + a^\dagger) \\ & + \hbar g_2 i \sigma_y (a^2 - (a^\dagger)^2). \end{aligned} \quad (A2)$$

Here we neglected terms of order $(g_0/\omega_0)^3$ and introduced the two coupling constants $g_1 = -g_0 \cos \zeta$ and $g_2 = -\frac{2g_0^2}{\omega_0} \sin \zeta \cos \zeta$ for one-photon and two-photon transitions, respectively. For the parameters used in the experiment the coupling g_2 is roughly two orders of magnitude smaller than the one photon coupling and below the semiclassical threshold for the two-photon lasing, $g_2^{\text{thr}} = \sqrt{\kappa^2 \Gamma_\varphi / (\Gamma_1 D_0^2)}$ [23]. In the parameters regime explored in the experiments, the Hamiltonian used in Eq. (1) gives thus a good description of the dynamics of the system.

-
- [1] E. Il'ichev *et al.*, Phys. Rev. Lett. **91**, 097906 (2003).
 - [2] A. Wallraff *et al.*, Nature **431**, 162 (2004).
 - [3] I. Chiorescu *et al.*, Nature **431**, 159 (2004).
 - [4] J. Johansson *et al.*, Phys. Rev. Lett. **96**, 127006 (2006).
 - [5] A. Naik *et al.*, Nature **443**, 193 (2006).
 - [6] D.I. Schuster *et al.*, Nature **445**, 515 (2007); A. A. Houck *et al.*, Nature **449**, 328 (2007).
 - [7] M. A. Sillanpää, J. I. Park, and R. W. Simmonds, Nature **449**, 438 (2007); J. Majer *et al.*, Nature **449**, 443 (2007).
 - [8] O. Astafiev *et al.*, Nature **449**, 588 (2007).
 - [9] M. Grajcar *et al.*, Nature Physics **4**, 612 (2008).
 - [10] A. Blais *et al.*, Phys. Rev. A, **69** 062320, (2004).
 - [11] D. A. Rodrigues, J. Imbers, and A. D. Armour Phys. Rev. Lett. **98**, 067204 (2007).
 - [12] J. Q. You *et al.*, Phys. Rev B **75**, 104516 (2007).
 - [13] J. Hauss *et al.*, Phys. Rev. Lett. **100**, 037003 (2008).
 - [14] M. Marthaler, G. Schön, and A. Shnirman Phys. Rev. Lett. **101**, 147001 (2008).
 - [15] O. V. Zhirov and D. L. Shepelyansky, Phys. Rev. Lett. **100**, 014101 (2008).
 - [16] H. Haken, *Laser Theory*, (Springer, Berlin, 1984).
 - [17] C. Cohen-Tannoudji, J. Dupont-Roc, and G. Grynberg, *Atom-Photon interactions*, (Wiley, New York, 1992).
 - [18] P. Mandel, Phys. Rev. A **21**, 2020 (1980).
 - [19] Y. Mu and C. M. Savage Phys. Rev. A **46**, 5944 (1992).
 - [20] C. Ginzel *et al.* Phys. Rev. A **48**, 732 (1993).
 - [21] O. Astafiev private communications.
 - [22] G. Falci *et al.*, Phys. Rev. Lett. **94**, 167002 (2005).
 - [23] Z. C. Wang and H. Haken Z. Phys. B **55**, 361 (1984).
 - [24] In Ref. [8], Astafiev *et al.* study the resonator spectrum as a function of the charging energy of the SSET and observe two bright spots, blue and red detuned with respect to the $\Delta = 0$ condition. We remark, that since in the experiment the Josephson energy is kept constant the detuning depends monotonically on the charging energy. Moreover a variation of the charging energy not only changes the detuning but also the coupling and the inversion. This does not change substantially the structure of the spectrum, but it leads to asymmetries between two peaks.